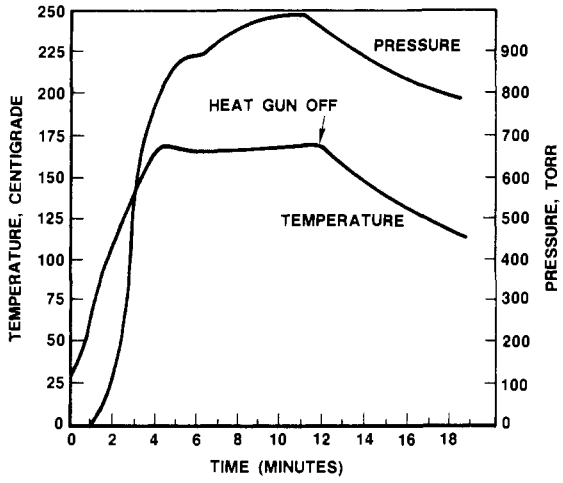

Figure 1. Pressure and temperature vs. time curves for the K_2NiF_6–BiF_5 system.

superatmospheric pressure, and there is no evidence for any reversible reactions. Furthermore, the F_2 is evolved at such moderate temperatures that reaction of the fluorine with the container walls is of no concern. The purity of the generated fluorine was shown to be in excess of 99% by its quantitative reaction with mercury.

Conclusion. Application of the same principle that was recently used for the chemical synthesis of elemental fluorine[6] to solid Lewis acids results in useful, solid-propellant-based, pure fluorine gas generators. The validity of the concept has been demonstrated for A_2MF_6 salts (A = K, Cs and M = Ni, Cu, Mn) and BiF_5 and TiF_4 as the Lewis acids. Further improvements in the attainable fluorine yields are anticipated by variation of the starting materials and Lewis acids and an optimization of the stoichiometries and reaction conditions.

Acknowledgment. We are grateful to Drs. L. R. Grant, C. J. Schack, and W. W. Wilson for their help and to the U.S. Army Research Office and the Office of Naval Research for partial financial support.

Registry No. K_2NiF_6, 17218-47-2; Cs_2CuF_6, 43070-30-0; Cs_2MnF_6, 16962-46-2; BiF_5, 7787-62-4; TiF_4, 7783-63-3; F_2, 7782-41-4.

Contribution from the Chemistry Department, University of California at San Diego, La Jolla, California 92093, and Department of Chemistry, University of Delaware, Newark, Delaware 19716

An Arbuzov-like Reaction in the Trimethyl Phosphite–η^2-Silaacyl Adduct $(\eta^5\text{-}C_5Me_5)Cl_3Ta\{\eta^2\text{-}OC(SiMe_3)[P(OMe)_3]\}$

John Arnold,† T. Don Tilley,*† Arnold L. Rheingold,*‡ and Steven J. Geib‡

Received November 19, 1986

Our studies concerning the carbonylation chemistry of early-transition-metal silyl complexes[1] have led to the discovery of $Cp^*Cl_3Ta(\eta^2\text{-}COSiMe_3)$ (**1**, $Cp^* = \eta^5\text{-}C_5Me_5$), a reactive η^2-silaacyl derivative.[1b,c] Recently we have found that **1** readily reacts with Lewis bases to form complexes of the type $Cp^*Cl_3Ta[\eta^2\text{-}OC(L)SiMe_3]$, in which the Lewis donor binds to the η^2-silaacyl carbon atom.[1c] Here we report the preparation and characterization of the trimethyl phosphite adduct $Cp^*Cl_3Ta\{\eta^2\text{-}OC(SiMe_3)[P(OMe)_3]\}$ (**2**) and its spontaneous Arbuzov-like dealkylation to MeCl and $Cp^*Cl_2Ta[\eta^4\text{-}OC(SiMe_3)P(OMe)_2O]$ (**6**). The latter compound, which has been characterized by X-ray crystallography, contains an unusual η^4-phosphonatosilaacyl(2–) ligand.

The dealkylation of trialkyl phosphites is promoted by a number of transition-metal complexes.[2] Dealkylation is usually preceded by coordination of phosphite to the transition metal. In a few cases this process appears to follow attack of the phosphite onto an electrophilic ligand bound to the metal,[3] as in the reaction reported here.

Results and Discussion

Silaacyl adduct $Cp^*Cl_3Ta\{\eta^2\text{-}OC[P(OMe)_3](SiMe_3)\}$ (**2**) is obtained upon addition of trimethyl phosphite to a benzene solution of the silaacyl $Cp^*Cl_3Ta(\eta^2\text{-}COSiMe_3)$[1c] (**1**, eq 1). A more

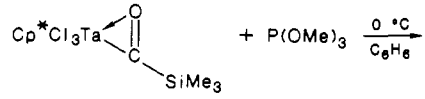

1

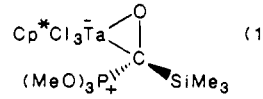

(1)

2

convenient method for the preparation of **2** involves pressurizing a pentane solution of $Cp^*Cl_3TaSiMe_3$[4] (**3**) and trimethyl phosphite (1:1) with 10–100 psi of carbon monoxide (eq 2). With a rapid,

$$\underset{\mathbf{3}}{Cp^*Cl_3TaSiMe_3} + P(OMe)_3 \xrightarrow[0\ ^\circ C,\ pentane]{CO} \mathbf{2} \qquad (2)$$

low-temperature workup (see Experimental Section), dark red crystals of **2** can be isolated in high yield.

Spectroscopic data indicate that **2** is structurally analogous to other silaacyl adducts, $Cp^*Cl_3Ta[\eta^2\text{-}OC(L)SiMe_3]$[1c,e] (**4**, L = pyridine; **5**, L = triethylphosphine). X-ray structures of the latter two compounds show that coordination of the Lewis base to the electron-deficient η^2-silaacyl results in reduction to an sp^3-hybridized carbon atom. Formation of these adducts is accompanied by a large upfield ^{13}C NMR chemical shift for the silaacyl carbon (δ 351) to δ 117.1 for **4**, δ 78.0 for **5**, and δ 103.1 for **2**.

Benzene-d_6 solutions of **2** change color from maroon to orange within a few minutes at 20 °C. Examination of ^1H NMR spectra of these solutions reveals shifts in the resonances for the C_5Me_5 (from δ 2.18 to 2.11) and $SiMe_3$ (from δ 0.15 to 0.49) groups and replacement of the doublet for the $P(OMe)_3$ group in **2** (δ 3.52, J_{PH} = 12.6 Hz) by a pair of doublets (δ 3.16, 3 H, J_{PH} = 11.1 Hz; δ 3.56, 3 H, J_{PH} = 10.8 Hz) and a singlet (δ 2.30, 3 H). The latter signal is due to MeCl, as determined by NMR and GC comparisons to an authentic sample. The remaining resonances are assigned to the new product **6**, isolated as orange crystals from a preparative-scale reaction (eq 3). Monitoring the reaction by ^{31}P NMR reveals gradual replacement of a singlet at δ 60.7 due to **2** by a peak at δ 36.6 for the Arbuzov reaction product **6**.

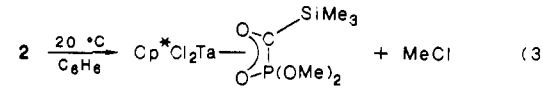

(3)

6

This reaction also occurs quantitatively in the solid state. Though slow at 22 °C under nitrogen, the reaction occurs rapidly

† UCSD.
‡ University of Delaware.

(1) (a) Tilley, T. D. *J. Am. Chem. Soc.* **1985**, *107*, 4084. (b) Arnold, J.; Tilley, T. D. *J. Am. Chem. Soc.* **1985**, *107*, 6409. (c) Arnold J.; Tilley, T. D.; Rheingold, A. L. *J. Am. Chem. Soc.* **1986**, *108*, 5355. (d) Campion, B. K.; Falk, J.; Tilley, T. D. *J. Am. Chem. Soc.* **1987**, *109*, 2049. (e) Arnold, J.; Tilley, T. D.; Rheingold, A. L.; Geib, S. J., manuscript in preparation.
(2) Brill, T. B.; Landon, S. J. *Chem. Rev.* **1984**, *84*, 577.
(3) (a) Baker, P. K.; Barker, G. K.; Green, M.; Welch, A. J. *J. Am. Chem. Soc.* **1980**, *102*, 7811. (b) Sweigart, D. A. *J. Chem. Soc., Chem. Commun.* **1980**, 1159. (c) Birch, A. J.; Jenkins, I. D.; Liepa, A. J. *Tetrahedron Lett.* **1975**, 1723.
(4) Arnold, J.; Shina, D. N.; Tilley, T. D.; Arif, A. M. *Organometallics* **1986**, *5*, 2037.

0020-1669/87/1326-2556$01.50/0

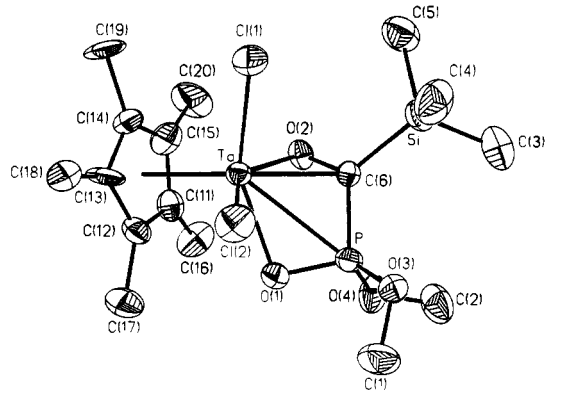

Figure 1. ORTEP view of **6** with atom-labeling scheme.

Table I. Crystal, Data Collection, and Refinement Parameters

(a) Crystal Parameters

formula	$C_{16}H_{31}O_4SiCl_2PTa$	γ, deg	80.40 (4)
cryst syst	triclinic	V, Å^3	1145 (1)
space group	$P\bar{1}$	Z	2
a, Å	9.266 (5)	ρ(calcd), g cm^{-3}	1.73
b, Å	11.217 (5)	temp, °C	23
c, Å	11.243 (5)	μ, cm^{-1}	54.2
α, deg	87.48 (4)	cryst dimens, mm	0.21 × 0.23 × 0.31
β, deg	83.99 (4)		

(b) Data Collection

diffractometer	Nicolet R3m/μ	no. of rflns collcd	4239
radiation	Mo Kα (λ = 0.71073 Å)	no. of unique data	4017
		no. of unique data, $4\sigma(F_o)$	3366
monochromator	graphite		
scan technique	Wyckoff	no. of std rflns	3 std/197 rflns
2θ scan range, deg	$4 \le 2\theta \le 50$	decay, %	≤1
data collcd	$\pm h,\pm k,+l$	R(int), %	1.96
scan speed, deg min^{-1}	variable 5–20	T(max)/T(min)	0.135/0.102

(c) Refinement

R_F, %	5.23	mean shift/esd max	0.126
R_{wF}, %	5.60	GOF	2.060
$\Delta(\rho)$, e Å^{-3}	2.30 (near Ta)	data/parameter	14.9
		g^a	0.001

$^a w^{-1} = \sigma^2(F_o) + gF_o^2$.

as **2** is heated in a melting point capillary tube. As the temperature is raised to ca. 90 °C, solid maroon **2** turns orange without melting. The melting point of this orange solid (101–103 °C) is just below that of pure **6** (108–110 °C). The ^{1}H NMR spectrum (benzene-d_6) of a sample of solid **2** that had been heated to 130 °C for 10 min under nitrogen was identical with that of pure **6** obtained from a solution thermolysis.

Presently, details concerning the mechanism of the conversion of **2** to **6** remain uncertain. It is possible that cleavage of the C–O bond in **2** is preceded by coordination of a phosphite methoxy group to tantalum. Displacement of a methyl group from **2** by chloride via an S_N2 process seems likely and could involve either a bimolecular pathway or prior dissociation of Cl^- from **2**. Formation of a strong Ta–O bond would facilitate displacement reactions that result in cleavage of the phosphite C–O bond. Although first-order plots of the reaction in eq 3 (monitored by ^{1}H NMR in benzene-d_6) gave straight lines for several half-lives, the rates derived from these data show a slight dependence on the initial concentration of **2**. Increasing $[\mathbf{2}]_{init}$ from 0.04 to 0.15 M brought about a rate increase from 1.6×10^{-3} to 3.7×10^{-3} s^{-1}. Although the rate data appear to be inconsistent with second-order kinetics, the slight participation of a bimolecular process cannot be excluded. Alternatively, increases in the polarity of the reaction solutions caused by increasing $[\mathbf{2}]_{init}$ may be responsible for changing the first-order rate constant in the observed manner.

Description of the Structure of 6. The structure of **6** consists of independent molecules with a central tantalum atom bonded to an η^5-C_5Me_5 ligand, two chlorides, and an η^4-phosphonatosilaacyl(2–) ligand. An ORTEP view is provided in Figure 1. Crystal and data collection parameters are summarized in Table I. Relevant geometrical parameters are given in Tables II–IV.

The Cp^*TaCl_2 metrical parameters are unexceptional, being comparable with those of $Cp^*TaCl_2(PhC{\equiv}CPh)$,[5] Cp^*TaCl_2-

Table II. Atomic Coordinates (×10^4) and Isotropic Thermal Parameters (Å^2 × 10^3) for **6**

	x	y	z	U^a
Ta	2261 (1)	2164 (1)	1961 (1)	33 (1)
Cl(1)	3735 (5)	451 (4)	2802 (1)	56 (1)
Cl(2)	4490 (5)	2527 (4)	759 (4)	59 (1)
P	2166 (4)	4512 (3)	2773 (3)	39 (1)
Si	3606 (5)	2758 (4)	4879 (4)	48 (1)
O(1)	1681 (11)	4124 (9)	1621 (9)	43 (3)
O(2)	1196 (10)	2587 (9)	3496 (8)	40 (3)
O(3)	3642 (12)	5022 (9)	2635 (9)	48 (4)
O(4)	900 (13)	5568 (11)	3212 (12)	65 (5)
C(1)	4073 (24)	5752 (19)	1584 (18)	77 (8)
C(2)	1035 (25)	6371 (21)	4108 (19)	81 (9)
C(3)	3313 (25)	4046 (22)	5900 (19)	83 (9)
C(4)	5590 (20)	2392 (19)	4328 (22)	79 (8)
C(5)	2957 (23)	1456 (19)	5735 (18)	75 (8)
C(6)	2477 (16)	3154 (12)	3573 (12)	36 (4)
C(11)	−91 (17)	2292 (15)	1230 (14)	48 (5)
C(12)	950 (18)	2237 (14)	189 (14)	48 (5)
C(13)	1808 (20)	1057 (15)	89 (14)	57 (6)
C(14)	1331 (20)	438 (13)	1111 (16)	54 (6)
C(15)	193 (19)	1144 (16)	1826 (17)	59 (6)
C(16)	−1329 (19)	3262 (18)	1573 (22)	74 (8)
C(17)	1024 (25)	3215 (18)	−742 (19)	77 (8)
C(18)	3003 (24)	604 (15)	−755 (17)	71 (8)
C(19)	1858 (28)	−876 (14)	1349 (23)	96 (11)
C(20)	−693 (26)	809 (23)	2946 (20)	93 (10)

^{a} Equivalent isotropic U defined as one-third of the trace of the orthogonalized U_{ij} tensor.

Table III. Selected Bond Distances and Angles

(a) Bond Distances (Å)

Ta–Cl(1)	2.384 (4)	P–O(1)	1.519 (11)
Ta–Cl(2)	2.430 (4)	P–O(3)	1.559 (12)
Ta–P	2.811 (4)	P–O(4)	1.577 (12)
Ta–O(1)	2.202 (9)	P–C(6)	1.732 (13)
Ta–O(2)	1.933 (9)	Si–C(3)	1.853 (24)
Ta–C(6)	2.210 (14)	Si–C(4)	1.861 (19)
Ta–C(11)	2.389 (16)	Si–C(5)	1.863 (22)
Ta–C(12)	2.431 (16)	Si–C(6)	1.886 (15)
Ta–C(13)	2.596 (17)	O(2)–C(6)	1.449 (18)
Ta–C(14)	2.510 (18)	O(3)–C(1)	1.467 (23)
Ta–C(15)	2.411 (19)	O(4)–C(2)	1.409 (27)
Ta–Ctr^a	2.155 (17)		

(b) Bond Angles (deg)

Cl(1)–Ta–Cl(2)	86.7 (1)	Ta–P–O(1)	51.1 (4)
Cl(1)–Ta–P	121.8 (1)	Ta–P–O(3)	116.8 (4)
Cl(2)–Ta–P	84.7 (1)	O(1)–P–O(3)	115.3 (6)
Cl(1)–Ta–O(1)	151.9 (3)	Ta–P–O(4)	134.9 (5)
Cl(2)–Ta–O(1)	80.6 (3)	O(1)–P–O(4)	103.8 (6)
P–Ta–O(1)	32.5 (3)	O(3)–P–O(4)	107.8 (6)
Cl(1)–Ta–O(2)	92.2 (3)	Ta–P–C(6)	51.9 (5)
Cl(2)–Ta–O(2)	139.4 (3)	O(1)–P–C(6)	102.1 (6)
P–Ta–O(2)	61.6 (3)	O(3)–P–C(6)	106.8 (7)
O(1)–Ta–O(2)	81.7 (4)	O(4)–P–C(6)	121.5 (7)
Cl(1)–Ta–C(6)	87.7 (3)	Ta–O(1)–P	96.4 (5)
Cl(2)–Ta–C(6)	99.2 (4)	Ta–O(2)–C(6)	80.2 (6)
P–Ta–C(6)	38.0 (3)	P–O(3)–C(1)	122.0 (12)
O(1)–Ta–C(6)	70.0 (4)	P–O(4)–C(2)	123.3 (13)
O(2)–Ta–C(6)	40.2 (5)	Ta–C(6)–P	90.1 (6)
Cl(1)–Ta–Ctr	105.4 (4)	Ta–C(6)–Si	132.6 (7)
Cl(2)–Ta–Ctr	110.7 (4)	P–C(6)–Si	128.6 (9)
P–Ta–Ctr	131.3 (4)	Ta–C(6)–O(2)	59.5 (6)
O(1)–Ta–Ctr	102.5 (5)	P–C(6)–O(2)	105.9 (9)
O(2)–Ta–Ctr	108.7 (5)	Si–C(6)–O(2)	119.4 (9)
C(6)–Ta–Ctr	147.8 (5)		

^{a} Ctr = Cp* ring centroid.

Table IV

Least-Squares Planes for **6**

atom	dev	atom	dev
Plane I: $0.7964X - 0.4527Y - 0.4011Z + 2.0269 = 0$			
O(1)	0.1590	P	−0.2657
O(2)	−0.1751	C(6)	0.2818
Plane II: $0.8484X + 0.2845Y + 0.4461Z - 3.6600 = 0$			
Ta	0.0	O(2)	0.0
O(1)	0.0		
Plane III: $0.6764X + 0.4284Y + 0.5991Z - 1.9475 = 0$			
C(11)	−0.0178	C(14)	0.0051
C(12)	0.0209	C(15)	0.0078
C(13)	−0.0160		

Dihedral Angles between Planes, deg

	II	III
I	68.4	84.0
II		15.6

(C_4H_8),[6] and $Cp^*TaCl_2(C_7H_{14})$.[6] The overall geometry resembles that found in cyclopentadienyl(diene)tantalum complexes such as $(\eta^5\text{-}C_5H_5)Ta(\eta^4\text{-}C_4H_6)Cl_2$.[7] The η^4-coordination of the phosphonatosilaacyl ligand results in a remarkably small bend angle between the O(1)–P–C(6)–O(2) and O(1)–Ta–O(2) planes (68.4°, Table IV). The corresponding angle in $(\eta^5\text{-}C_5H_5)Ta(\eta^4\text{-}C_4H_6)Cl_2$ is 94.9°.[7] The parameters associated with the TaOC triangle are similar to those in the related compounds **4** and **5**. For example, the Ta–C(6) distance in **6** (2.21 (1) Å) compares with the analogous distances in **4** (2.214 (5) Å) and **5** (2.24 (2) Å) and is typical for a Ta(V)–C single bond.[6] The C–O distance in **6** (1.45 (2) Å) is slightly longer than in **4** and **5** (1.416 (6) and 1.43 (3) Å, respectively). The angles within the TaOC triangles are identical, within experimental error, for **4**, **5**, and **6**. These comparisons suggest contributions from resonance hybrids B and C; other resonance structures may also be considered:

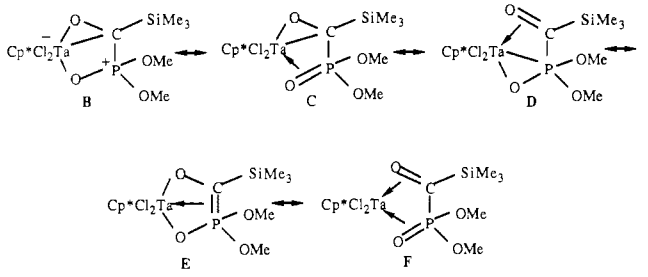

The Ta–P distance (2.811 (4) Å) is slightly longer than Ta–P distances found in tantalum(V) phosphine complexes (2.5–2.6 Å).[8] At 1.73 (1) Å, the C(6)–P distance is shorter than typical C–P single bonds (ca. 1.8 Å) but is consistent with C–P distances found in phosphorus ylides (structure E).[9] The P–O(1) distance (1.52 (1) Å) is shorter than the remaining P–O distances (average 1.57 (1) Å) and may reflect a degree of P=O character (resonance structures C and F). Coordination of O(1) to tantalum distorts the angles around the phosphonato group such that C(6)–P–O(1) is the smallest of the three C–P–O angles. Of the two Ta–O bonds, the one from the phosphonato oxygen is the longest (2.202 (9) Å for Ta–O(1); 1.933 (9) Å for Ta–O(2)). On the basis of the above structural parameters, it appears that there is considerable delocalization of electron density in the η^4-phosphonatosilaacyl(2−) ligand, leading to a number of contributing resonance forms with structure C being perhaps most important.

Experimental Section

Manipulations were performed under an atmosphere of nitrogen or argon by using Schlenk techniques or in a Vacuum Atmospheres glovebox. Dry, oxygen-free solvents were employed throughout. Elemental analyses were performed by Galbraith Laboratories. Infrared spectra were recorded on a Perkin-Elmer 1330 spectrometer. NMR spectra were recorded with a GE-QE-300 instrument at 300, 122, or 75.5 MHz (^1H, ^{31}P, and ^{13}C respectively) and at 90 MHz on a Varian EM 390 (^1H). GC analyses were conducted with a Varian 3400 instrument utilizing a Varian 4290 integrating recorder. A 3 m × $^1/_8$ in. stainless-steel column with 25% 1,2,3-tris(2-cyanoethoxy)propane as stationary phase was employed. Carbon monoxide (Liquid Carbonics) and 90% ^{13}C carbon monoxide (MSD) were used as received. Trimethyl phosphite (Aldrich) was dried over 5-Å sieves and vacuum-transferred before use.

$Cp^*Cl_3Ta\{\eta^2\text{-}OC(SiMe_3)[P(OMe)_3]\}$ (2). A green solution of **3** (0.03 g, 0.60 mmol) and $P(OMe)_3$ (0.24 mL, excess) in pentane (20 mL) was cooled to 0 °C and pressurized with CO (100 psi). After being stirred for 10 min, the maroon solution was evaporated under dynamic vacuum, and the sticky residue was dissolved in cold ether (20 mL at 0 °C). The solution was quickly filtered, concentrated to 5 mL, and cooled to −45 °C. After 8 h, dark red crystals (0.29 g, 74%) were isolated by filtration. Anal. Calcd for $C_{17}H_{33}Cl_3O_4SiTa$: C, 31.5, H, 5.13; P, 4.78. Found: C, 32.1; H, 5.15; P, 4.47. IR (Nujol mull, CsI, cm^{-1}): 2709 w, 1485 m, 1258 m, 1241 s, 1182 m, 1135 w, 1076 s, 1040 s, 1030 s, 992 s, 870 s, 829 s, 744 m, 688 m, 665 m, 526 m, 464 w, 390 w, 367 m, 318 s, 285 s. ^1H NMR (benzene-d_6, 90 MHz, 34 °C): δ 0.15 (s, 9 H, $SiMe_3$), 2.18 (s, 15 H, C_5Me_5), 3.52 (d, J_{PH} = 12.6 Hz, 9 H, $P(OMe)_3$). $^{13}C\{^1H\}$ NMR (with sample obtained by using ^{13}CO (90% ^{13}C), toluene-d_8, 75.5 MHz, −60 °C): δ 103.1 (d, J_{PC} = 158 Hz, $OC[P(OMe_3)_3]$). $^{31}P\{^1H\}$ NMR (benzene-d_6, 122 MHz, 20 °C): δ 60.70 (s, $P(OMe)_3$).

$Cp^*Cl_2Ta[\eta^4\text{-}OC(SiMe_3)P(OMe)_2O]$ (6). (a) Compound **3** (0.50 g, 1.0 mmol), $P(OMe)_3$ (0.25 mL, excess), and pentane (30 mL) were stirred together for 15 min under a CO atmosphere (100 psi). The volatiles were removed by evacuation, and the dark red residue was dissolved in benzene (20 mL). After 3 h, the yellow solution that had formed was pumped down to give a yellow oil. Extraction with pentane (2 × 20 mL), concentration of the combined pentane extracts to ca. 5 mL, and cooling (−45 °C, 8 h) produced 0.50 g (84%) of orange crystals (mp 108–110 °C). Anal. Calcd for $C_{16}H_{30}Cl_2O_4PSiTa$: C, 32.2; H, 5.06; Cl, 11.9. Found: C, 32.6; H, 5.20; Cl, 11.8. IR (Nujol mull, CsI, cm^{-1}): 2720 w, 1242 s, 1173 m, 1077 s, 1061 s, 1042 s, 1020 s, 968 m, 845 s, 829 s, 768 s, 746 w, 683 w, 640 m, 621 m, 586 m, 535 m, 480 m, 356 m, 314 m, 268 m. ^1H NMR (benzene-d_6, 300 MHz, 20 °C): δ 0.49 (s, 9 H, $SiMe_3$), 2.11 (s, 15 H, C_5Me_5), 3.16 (d, J_{PH} = 11.1 Hz, 3 H, $P(OMe)_2$), 3.56 (d, J_{PH} = 10.8 Hz, 3 H, $P(OMe)_2$). $^{13}C\{^1H\}$ NMR (benzene-d_6, 75.5 MHz, 20 °C): δ 0.27 ($SiMe_3$), 11.08 (C_5Me_5), 53.08 (d, J_{PC} = 6 Hz, $P(OMe)_2$), 55.67 (d, J_{PC} = 9 Hz, $P(OMe)_2$), 79.41 (d, J_{PC} = 104 Hz, $OCSiMe_3$), 125.7 (C_5Me_5). $^{31}P\{^1H\}$ NMR (benzene-d_6, 122 MHz, 20 °C): δ 36.50 (s, $P(OMe)_2$).

(b) Complex **2** (0.020 g) was heated to 130 °C for 10 min under a nitrogen atmosphere in a rubber-septum-capped 5-mm NMR tube. Addition of benzene-d_6 (0.4 mL) (via syringe) to the resulting orange residue gave a homogeneous orange solution that contained **6** and MeCl (1:1) as the only identifiable products by ^1H NMR.

Collection of Diffraction Data. Crystal data and parameters used during the collection of diffraction data are contained in Table I. An orange, irregular crystal of **6** was sealed in a glass capillary tube. Preliminary photographic evidence revealed no symmetry higher than triclinic. Unit-cell dimensions were derived from the least-squares fit of the angular settings of 24 reflections with $20° < 2\theta < 25°$. Data were corrected for absorption by an empirical procedure that employs six refined parameters to define a pseudoellipsoid used to calculate the corrections. The centrosymmetric alternative $P\bar{1}$ was initially assigned and later verified by the refinement results.

Solution and Refinement of 6. The Ta atom was located from a Patterson map. The remaining non-hydrogen atoms were located from subsequent difference Fourier syntheses. Non-hydrogen atoms were refined anisotropically. Hydrogen atom positions were calculated and fixed in idealized positions (d(C–H) = 0.96 Å, thermal parameters equal 1.2 times the isotropic equivalent for the carbon atom to which it was attached). An inspection of F_o vs. F_c values and trends based upon sin θ, Miller index, or parity group failed to reveal any systematic error in the data. All computer programs used in the data collection and refinement are contained in the Nicolet program packages P3 and SHELXTL (version 5.1).

(5) Smith, G.; Schrock, R. R.; Churchill, M. R.; Youngs, W. J. *Inorg. Chem.* **1981**, *20*, 387.
(6) Churchill, M. R.; Youngs, W. J. *J. Am. Chem. Soc.* **1979**, *101*, 6462.
(7) Yasuda, H; Tatsumi, K.; Okamoto, T.; Mashima, K.; Lee, K.; Nakamura, A.; Kai, Y.; Kanehisa, N.; Kasai, N. *J. Am. Chem. Soc.* **1985**, *107*, 2410.
(8) (a) Churchill, M. R.; Wasserman, H. J.; Turner, H. W.; Schrock, R. R. *J. Am. Chem. Soc.* **1982**, *104*, 1710. (b) Mayer, J. M.; Wolczanski, P. T.; Santarsiero, B. D.; Olson, W. A.; Bercaw, J. E. *Inorg. Chem.* **1983**, *22*, 1150. (c) Fellmann, J. D.; Rupprecht, G. A.; Wood, C. D.; Schrock, R. R. *J. Am. Chem. Soc.* **1978**, *100*, 5964.
(9) (a) Johnson, W. A. *Ylid Chemistry*; Academic: New York, 1966. (b) Moloy, K. G.; Marks, T. J.; Day, V. W. *J. Am. Chem. Soc.* **1983**, *105*, 5696.

Atomic coordinates are provided in Table II, selected bond distances and angles in Table III, and least-squares planar calculations in Table IV. Additional data are available as supplementary material.

Acknowledgment is made to the Air Force Office of Scientific Research, Air Force Systems Command, USAF, for support of this work under Grant No. AFOSR-85-0228.

Supplementary Material Available: Tables of bond distances and angles, anisotropic temperature factors, and hydrogen atom coordinates (4 pages); a listing of calculated and observed structure factors (20 pages). Ordering information is given on any current masthead page.

Contribution from the Departments of Chemistry, Yale University, New Haven, Connecticut 06511, and Oklahoma State University, Stillwater, Oklahoma 74078

Chelation of a C–F Bond to Iridium in an 8-Fluoroquinoline Complex

Robert J. Kulawiec, Elizabeth M. Holt,* Maryellen Lavin, and Robert H. Crabtree*

Received January 23, 1987

We have previously shown that cationic iridium(I)[1] and -(III)[2] complexes can bind the lone pairs of iodo-, bromo- and chlorocarbons to give complexes. In each case the M–X distance is equal to the sum of the covalent radii and the angle C–X–M is near 102°. This angle is, we believe, consistent with binding to the largely p-type lone pairs on the halogen. Fluorocarbons such as *o*-C_6H_4BrF did not bind via the C–F bond in analogous systems.[2] We were therefore prompted to use 8-fluoroquinoline, because we had previously found[3] that 8-methylquinoline gives the agostic system $[IrH_2L_2(8\text{-}MeC_9H_6N)]^+$, in a case where the corresponding methane complex is unknown.

Beck has given IR evidence[4] for halocarbon binding to various transition-metal cations; Uson, Cotton, et al. have reported a bromocarbon[5] and fluorocarbon[6] example, and Richards has a fluorocarbon case.[7]

Results and Discussion

Hydrogenation of $[Ir(cod)(PPh_3)_2]SbF_6$ (cod = 1,5-cyclooctadiene) in the presence of weakly binding ligands, S, has proved to be an effective way of making the complexes $[IrH_2L_2S_2]^+$ (S = Me_2CO, tetrahydrofuran (thf), H_2O, MeI, and MeCN).[8] We therefore performed this reaction in the presence of 8-fluoroquinoline. The greenish white product was purified by recrystallization from CH_2Cl_2–Et_2O and characterized by IR and ^1H, ^{19}F, and ^{31}P NMR spectroscopy and, in particular, by an X-ray crystallographic study.

We will first discuss the spectral studies. The ^1H NMR spectrum of the product shows two hydride resonances, H_A at δ −19.5 and H_B at δ −39.3. Each shows coupling to two cis PPh_3 groups ($^2J(P,H(cis))$ = 16.5 Hz (H_A) and 15.3 Hz (H_B)) as appropriate for a cis arrangement of these ligands. The two hydrogens are present in the same molecule as shown by the H,H coupling ($^2J(H,H')$ = 10.3 Hz), as we often find in such complexes. Significantly, only H_B shows coupling to ^{19}F ($^2J(H,F(trans))$ = 95 Hz), suggesting that H_B is trans to F. Larger coupling between trans ligands is a common feature of transition-metal complexes,[9] but the rarity of hydrido fluorides[10] means that no cases of trans H,F coupling have been reported. The resonances for the PPh_3 and fluoroquinoline ligands are normal.

In acetone-d_6, the fluoroquinoline is displaced to give $[IrH_2L_2S_2]^+$ (S = Me_2CO), showing the high coordinative lability of the quinoline ligand. Conversely, the isolated acetone complex will react in CD_2Cl_2 with the fluoroquinoline to re-form the chelate complex.

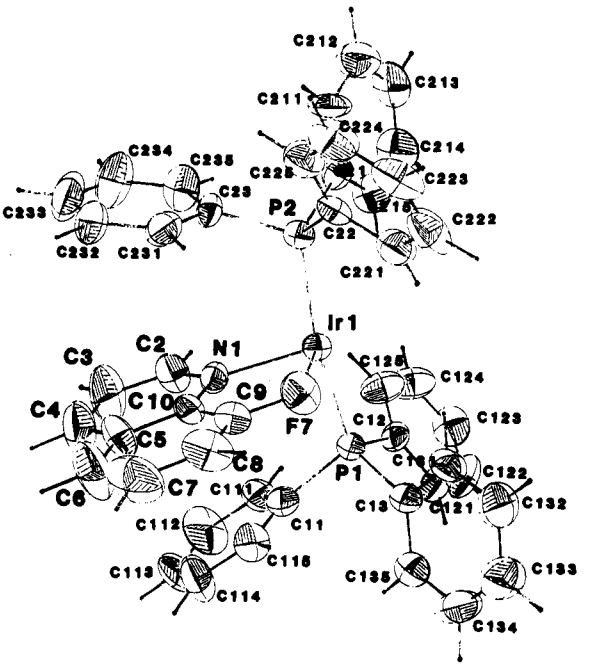

Figure 1.

Table I. Crystal Data for $IrSbP_2F_7NC_{45}H_{38}$[a]

formula	$IrSbP_2F_7NC_{45}H_{38}$	λ(Mo Kα)	0.710 69 Å
M_r	1087.7	D_{calcd}	1.710 g cm^{-3}
a	11.904 (7) Å	Z	4
b	19.891 (11) Å	obsd reflcns	5114
c	18.213 (4) Å	R	5.5%
β	101.63 (4)°	R_w	7.0%
V	4223.9 (37) Å^3	space group	$P2_1/c$
F(000)	2116	scan rate	variable
μ(Mo Kα)	39.14 cm^{-1}	scan type	θ–2θ

[a] Obtained on a Syntex P3 diffractometer.

The ^{19}F NMR spectrum shows a resonance centered at δ −172 from the $CFCl_3$ standard. The coupling to H_B is clearly resolved ($^2J(F,H)$ = 100 Hz), but for its exact value, we prefer to trust the ^1H NMR signal, which was better resolved. The chelated fluorine showed a coordination shift of −46 ppm relative to the resonance for free 8-fluoroquinoline at δ −126.

The IR spectrum of the complex shows a strong band at 1231.6 cm^{-1}, which we identify as the C–F stretching frequency. Aryl C–F vibrations have been reported in the range 1100–1250 cm^{-1}.[11] The coordination shift from free 8-fluoroquinoline (ν(C–F) = 1245.7 cm^{-1} (s)) is −14 cm^{-1}. The interaction therefore probably

* To whom correspondence should be addressed: E.M.H., Oklahoma State University; R.H.C., Yale University.

(1) Burk, M. J.; Crabtree, R. H.; Holt, E. M. *Organometallics* **1984**, *3*, 638.
(2) Crabtree, R. H.; Faller, J. W.; Mellea, M. F.; Quirk, J. M. *Organometallics* **1982**, *1*, 1361.
(3) Crabtree, R. H.; Holt, E. M.; Lavin, M. E.; Morehouse, S. M. *Inorg. Chem.* **1985**, *24*, 1986.
(4) Beck, W.; Schloter, K. *Z. Naturforsch, B: Anorg. Chem. Org. Chem.* **1978**, *33B*, 1214.
(5) Cotton, F. A.; Lahuerta, P.; Sanau, M.; Schwotzer, W.; Solava, I. *Inorg. Chem.* **1986**, *25*, 3526.
(6) Uson, R.; Fornies, J.; Tomas, M.; Cotton, F. A.; Falvello, L. R. *J. Am. Chem. Soc.* **1984**, *106*, 2482.
(7) Catala, R. M.; Cruz-Garritz, D.; Hills, A.; Hughes, D. L.; Richards, R. L.; Sosa, P.; Torrens, H., personal communication, 1986.
(8) Crabtree, R. H.; Demou, P. C.; Eden, D.; Mihelcic, J. M.; Parnell, C. A.; Quirk, J. M.; Morris, G. E. *J. Am. Chem. Soc.* **1982**, *104*, 6884.
(9) Lukehart, C. M. *Fundamental Transition Metal Organometallic Chemistry*; Brooks/Cole: Belmont, CA, 1985.
(10) Crabtree, R. H.; Hlatky, G. G.; Holt, E. M. *J. Am. Chem. Soc.* **1983**, *105*, 7302.
(11) Pavia, D. L.; Campman, G. M.; Kriz, G. S. *Introduction to Spectroscopy*; Saunders: Philadelphia, 1979; p 72.

0020-1669/87/1326-2559$01.50/0